Makara Journal of Science

Volume 20
Issue 3 *September*

Article 4

9-20-2016

Extraction of the Proton Charge Radius from Experiments

Neelima Govind Kelkar
Departamento de Física, Universidad de los Andes, Cra.1E No.18A-10, Santafe de Bogotá, Colombia, nkelkar@uniandes.edu.co

Terry Mart
Department of Physics, Faculty of Mathematics and Natural Sciences, Universitas Indonesia, Depok 16424, Indonesia

Marek Nowakowski
Departamento de Física, Universidad de los Andes, Cra.1E No.18A-10, Santafe de Bogotá, Colombia

Extraction of the Proton Charge Radius from Experiments

Cover Page Footnote

T.M. was supported by the Research-Cluster-GrantProgram of the University of Indonesia, under Contract No. 1862/UN.R12/HKP.05.00/2015.

Makara Journal of Science, 20/3 (2016), 119-126
doi: 10.7454/mss.v20i3.6242

MINI-REVIEW

Extraction of the Proton Charge Radius from Experiments

Neelima Govind Kelkar[1*], Terry Mart[2], and Marek Nowakowski[1]

1. Departamento de Física, Universidad de los Andes, Cra.1E No.18A-10, Santafe de Bogotá, Colombia
2. Department of Physics, Faculty of Mathematics and Natural Sciences, Universitas Indonesia, Depok 16424, Indonesia

[*]*E-mail: nkelkar@uniandes.edu.co*

Received June 15, 2016 | Accepted August 26, 2016

Abstract

The static properties of hadrons, such as their radii and other moments of the electric and magnetic distributions, can only be extracted using theoretical methods and cannot be directly measured from experiments. As a result, discrepancies between the extracted values from different precision measurements can exist. The proton charge radius, r_p, which is extracted either from electron-proton (*e-p*) elastic scattering data or from hydrogen atom spectroscopy, seems to be no exception. The value r_p = 0.84087(39) fm extracted from muonic hydrogen spectroscopy is about 4% smaller than that obtained from *e-p* scattering or standard hydrogen spectroscopy. The resolution of this so-called proton radius puzzle has been attempted in many different ways over the past six years. The present article reviews these attempts with a focus on the methods of extracting the radius.

Abstrak

Ekstraksi Radius Muatan Proton dari Eksperimen. Sifat-sifat statik hadron seperti radius serta momen-momen lain dari distribusi listrik dan magnetik hanya dapat diekstrak melalui metode teoretis dan tidak dapat langsung diukur melalui eksperimen. Akibatnya, perbedaan antara nilai-nilai yang diekstrak dari pelbagai pengukuran berbeda sering terjadi. Radius muatan dari proton, r_p, yang diekstrak dari data hamburan elastik elektron proton atau dari spektroskopi atom hidrogen merupakan salah satu contoh problem ini. Nilai r_p = 0.84087(39) fm yang diekstrak dari spektroskopi hidrogen muonik diketahui 4% lebih kecil dibandingkan dengan nilai yang diperoleh dari hamburan elastik elektron proton atau pun dari spektroskopi hidrogen baku. Pemecahan masalah yang sering disebut teka-teki radius proton ini sudah banyak dicoba dengan menggunakan pelbagai cara selama enam tahun terakhir. Makalah ini mengulas usaha-usaha tersebut dengan fokus metode ekstraksi radius.

Keywords: electron-proton scattering, proton; radius, Zeemach moment

Introduction

The structure of the proton plays an important role in atomic physics, where experiments have reached a very high level of precision. The inclusion of the proton structure is critical to the accurate comparison of experimentally measured transition energies and very precise quantum electrodynamics (QED) calculations. Conversely, the unprecedented precision of atomic physics experiments makes it possible to probe some of the static properties of the proton, such as its radius. Properties such as its charge and magnetization density are usually obtained as Fourier transforms of the Sachs form factors [1-4] that are extracted from electron-proton (*e-p*) scattering cross-section measurements. One can deduce the radius and other moments from these densities and infer the size of the proton. The radius thus extracted from *e-p* scattering and hydrogen spectroscopy seemed to be commensurate within error bars until a recent precision measurement of transition energies in muonic hydrogen suggested otherwise. Surprisingly, a comparison of the theoretical calculation of the Lamb shift in muonic hydrogen, including all QED and finite-size corrections (FSC), with the very precisely measured value of the shift $\Delta E = E^{f=2}_{2P_{3/2}} - E^{f=1}_{2S_{1/2}} = 206.2949(32)$ meV in muonic hydrogen, led to a radius which was 4% smaller than the average CODATA (Committee on data for Science and Technology) value of 0.8768(69) fm [5,6]. The extracted value of r_p = 0.84184(67) fm was much more accurate than the previous ones. This so-called “proton puzzle”

was later reinforced [7,8] with the precise value of r_p = 0.84087(39) fm from muonic hydrogen spectroscopy.

The puzzle gave rise to extensive literature that attempted solutions involving different approaches for the evaluation of FSC [9], off-shell correction to the photon-proton vertex [10,11], the charge density being poorly constrained by data [12], and the existence of non-identical protons [13], as well as difficulties in choosing the reference frame in the extraction of the radius [14-16]. On the experimental side, accurate spectroscopic measurements of muonic deuterium and helium transition energies as well as additional scattering experiments are expected to shed light on the problem. For details of these plans, we refer the reader to Refs. [17,18]. The present article will focus on the theoretical aspects and the possible discrepancies arising from the methods used for the extraction of the proton radius.

Proton charge radius and other moments

The size (or extension) of the proton is characterized by the moments of its charge density, ρ_p as

$$\left\langle r^m \right\rangle = \int r^m \rho_p(r)\, d^3r \,. \tag{1}$$

The charge density is conventionally defined as the Fourier transform of the electric form factor, $G_E^p(\boldsymbol{q}^2)$, namely, $G_E^p(\boldsymbol{q}^2) = \int e^{-i\boldsymbol{q}\cdot\boldsymbol{r}} \rho_p(\boldsymbol{r})\, d^3r/(2\pi)^3$. Starting with this Fourier transform,

$$\begin{aligned} G_E^p(\boldsymbol{q}^2) &= \frac{1}{2\pi^2}\int_0^\infty r^2 \rho_p(r) \frac{\sin(|\boldsymbol{q}|\,r)}{|\boldsymbol{q}|\,r} dr \\ &= \frac{1}{2\pi^2}\int_0^\infty r\rho_p(r)\left[|\boldsymbol{q}|\,r - \frac{|\boldsymbol{q}|^3 r^3}{6} + \ldots\right] dr \\ &= \frac{1}{2\pi^2}\int_0^\infty r^2 \rho_p(r)\, dr - \frac{1}{2\pi^2}\frac{|\boldsymbol{q}|}{6}\int_0^\infty r^4 \rho_p(r)\, dr + \ldots \end{aligned} \tag{2}$$

it is easy to see that the radius defined above as $\left\langle r_p^2 \right\rangle = \int r^2 \rho_p(r)\, d^3r$ can also be expressed in terms of the form factor $G_E^p(\boldsymbol{q}^2)$ as

$$-\frac{6}{G_E^p(0)}\frac{dG_E^p(\boldsymbol{q}^2)}{d\boldsymbol{q}^2}\bigg|_{\boldsymbol{q}^2=0} = \left\langle r_p^2 \right\rangle. \tag{3}$$

There exists another approach in order to extract the proton radius from experiments, one involving atomic spectroscopy. In this approach, one attempts to calculate the theoretical difference between atomic energy levels with the inclusion of all possible corrections from QED as well as the proton FSC. This difference is then compared with the experimentally measured transition energies in order to fit the radius that appears in the theoretical expression due to the inclusion of FSC. Such an approach was used in [7,8], and, apart from the second moment of the charge density, the FSC in Ref. [7,8] also included the third Zemach moment [19] defined by

$$\left\langle r^3 \right\rangle_2 = \int d^3r\, r^3 \rho_{(2)}(r) \tag{4}$$

where $\rho_2(r) = \int d^3z\, \rho_p(|\,\boldsymbol{z}-\boldsymbol{r}\,|)\, \rho_p(z)$. This inclusion introduced a small model dependence in the extraction and has been discussed at length by several authors [20-23]. Some uncertainty depending on the approach for including the FSC was also found in Ref. [9].

Breit frame, Lorentz boost, and relativistic corrections

In order to compare the radius extracted from the two methods mentioned in the previous subsection, we must ensure that the extractions are done in the same frame of reference. As mentioned in Ref. [24], the size and shape of an object are not relativistically invariant quantities: observers in different frames will infer different magnitudes for these quantities. The static relation $\left\langle r_p^2 \right\rangle = \int r^2 \rho_p(r)\, d^3r$ defines the radius in the rest frame of the proton. The extraction of the radius from *e-p* scattering is, however, not done in the proton rest frame. The *e-p* scattering data is used to extract the invariant form factor $G_E(\boldsymbol{q}^2)$, where the four-momentum transfer squared in *ep* elastic scattering is $q^2 = \omega^2 - \boldsymbol{q}^2$. The radius is then evaluated using the following relation [25]:

$$\left\langle r_p^2 \right\rangle = -\frac{6}{G_E^p(0)}\frac{dG_E^p(q^2)}{dq^2}\bigg|_{q^2=0} \tag{5}$$

This definition looks slightly different from that derived in Eq. (3), with the three-momentum transfer being replaced by the four-momentum transfer squared in Eq. (5). At first sight, Eq. (5) has the appearance of a Lorentz invariant quantity (and this appearance has even misled some authors to believe so [26]). However, if we examine the condition $q^2 = 0$, with $q^2 = \omega^2 - \boldsymbol{q}^2$, it either means that $\omega^2 = \boldsymbol{q}^2 \neq 0$ (in which case we have a real photon) or $\omega = |\,\boldsymbol{q}\,| = 0$. It is impossible to exchange a real photon in the *t*-channel exchange diagram in elastic *e-p* scattering, so we have to drop the first possibility. The second choice involving $\omega = 0$ is, however, equivalent to choosing the Breit or the so-called brick-wall frame, in which the sum of the initial and final proton momentum is zero. This interpretation is consistent with what we find in the Breit equation where the same reference frame has to be chosen. The radius extracted in this frame should then be boosted to the proton rest frame before comparing it with the one extracted from atomic spectroscopy [14]. This and other relativistic corrections become important [14] with the improved precision of experimental data. Finally, we would like to comment that the extraction of the proton radius from atomic spectroscopy relies on formulas that start with the definition of the radius as given in Eq. (1).

The form factor $G_E^p(\boldsymbol{q}^2)$ is a Fourier transform of the density $\rho_p(r)$ in the rest frame, and hence this form factor is $G_E^p(\boldsymbol{q}^2) = G_E^p(q^2)$ in the non-relativistic case but $G_E^p(\boldsymbol{q}^2) \neq G_E^p(q^2)$ in the relativistic case. There have been several attempts in the literature to incorporate the above relations with relativistic corrections [27-31]. The fact that the structure of a bound system is independent of its motion in the non-relativistic case, whereas it changes in the relativistic case depending on how fast it moves, was taken into account in [32] for the calculation of the deuteron radius as well. The authors in [14] found that incorporating the relativistic corrections (along with the Lorentz boost) could indeed remove the 4% discrepancy between the *e-p* scattering and μ-*p* Lamb shift determinations of the radius.

Finite-size effects

The corrections to the energy levels at order α^4 due to the structure of the proton are generally included using first-order perturbation theory with the point-like Coulomb potential modified by the inclusion of form factors [9]. The determination of the proton radius from accurate Lamb shift measurements in Ref. [7,8] relies for the FSC on a seminal calculation of Friar [33] based on a third-order perturbation expansion of the energy that leads to an expression that depends on the proton radius rather than the form factors explicitly. Such an expression is a result of approximating the atomic wave function everywhere by its value at its center and is useful in extracting the radius from spectroscopic measurements. In Ref. [33], the author finds

$$\Delta E \approx \langle 0|\Delta V|0\rangle + \langle 0|\Delta V|\Delta\phi\rangle + \langle \Delta\phi|\Delta V|\Delta\phi\rangle - \langle 0|\Delta V|0\rangle\langle\Delta\phi|\Delta\phi\rangle \quad (6)$$

where ΔV is the perturbation and the wave function $|\Psi\rangle = |0\rangle + |\Delta\phi\rangle$, with $|0\rangle$ and $|\Delta\phi\rangle$ the unperturbed part and the first-order perturbation, respectively. Further, approximating the wave function $\Phi_n(r) = \langle \mathbf{r}|0\rangle$ by its value at $r = 0$,

$$\Delta E_{\rm FSC} \approx \frac{2\pi\alpha Z}{3}|\Phi_n(0)|^2\left[\langle r^2\rangle - \frac{\alpha Z m_r}{2}\langle r^3\rangle_{(2)} + \ldots\right] \quad (7)$$

The second term involves the third Zemach moment given by Eq. (4), which can be rewritten in terms of $\langle r_p^2\rangle$ as

$$\langle r^3\rangle_{(2)} = \frac{48}{\pi}\int_0^\infty \frac{dq}{q^4}\left[G_E^{p2}(q^2) - 1 + q^2\frac{\langle r_p^2\rangle}{3}\right] \quad (8)$$

The extraction of the radius from the muonic Lamb shift [3] was done using the above relation with a dipole form for $G_E(q^2)$ in order to rewrite $\langle r^3\rangle_2$ in Eq. (7) in terms of $\langle r_p^2\rangle$. Replacing all coefficients in Eq. (7) and including all QED corrections, the final expressions used in the two references in Ref. [3] in order to compare with the experimental values of

$\Delta E(= E^{f=1}_{2S_{1/2}} - E^{f=2}_{2P_{3/2}}) = 206.2949(32)$ meV and

$\Delta E_L(= E_{2P_{1/2}} - E_{2S_{1/2}}) = 202.3706(23)$ meV, where

$$\begin{aligned}\Delta E(= E^{f=1}_{2S_{1/2}} - E^{f=2}_{2P_{3/2}}) &= 209.9779(49) - 5.2262r_p^2 + 0.0347r_p^3 \text{ meV}\\ \Delta E_L(= E_{2P_{1/2}} - E_{2S_{1/2}}) &= 206.0336(15) - 5.2275(10)r_p^2 + \Delta E_{TPE} \text{ meV}\end{aligned} \quad (9)$$

where the last term corresponds to the full two-photon exchange (TPE) contribution [34]. Note that the $\langle r^3\rangle_2$ term in Friar's expression of Eq. (7) is an order α^5 correction and corresponds in principle to a TPE diagram as shown in Ref. [35]. In order to confirm that the above formula [Eq. (9)], which relies on perturbative methods and is used to fit the proton radius, does not change significantly due to the use of nonperturbative methods, the authors in Ref. [36] calculated the transition energies by numerically solving the Dirac equation, including the finite-size Coulomb interaction and finite-size vacuum polarization. The point-like Coulomb potential was replaced by one including the proton charge distribution, $\rho(r)$, given by

$$V_C(r) = -\frac{Z\alpha}{r} \to -Z\alpha\int\frac{\rho(r')}{|\mathbf{r}-\mathbf{r}'|}d^3r';\ \rho(r) = \frac{\eta}{8\pi}e^{-\eta r};\ \eta = \sqrt{\frac{12}{\langle r_p^2\rangle}} \quad (10)$$

The energy shift was calculated by taking the difference between the eigenvalues calculated using the Dirac equation with the above potential for several values of $\langle r_p^2\rangle$. These energy shifts were then interpolated and fitted to the function $f = A\langle r_p^2\rangle + B\langle r_p^2\rangle^{3/2}$ in order to determine the coefficients *A* and *B*. Their final result, namely,

$$\Delta E(= E^{f=1}_{2S_{1/2}} - E^{f=2}_{2P_{3/2}}) = 209.9505 - 5.2345r_p^2 + 0.0361r_p^3 \text{ meV} \quad (11)$$

as compared to Eq. (9), led to a radius which differed from the central value of 0.84184(67) fm but was well within the error bars. Thus, no significant discrepancy between perturbative and nonperturbative methods was found. However, the authors in Ref. [37], on solving the Schrödinger equation numerically, found that the difference between the perturbative methods and nonperturbative numerical calculations of the 2*S*

hyperfine splitting in muonic hydrogen was larger than the experimental precision.

A different relativistic approach for the FSC based on the Breit equation with form factors was investigated in Ref. [9]. The method relies on the fact that all ***r***-dependent potentials in quantum field theory (QFT) are obtained by Fourier transforming an elastic scattering amplitude suitably expanded in $1/c^2$. The Breit equation [38-42] follows the very same principle for elastic $e^-\mu^+$, e^+e^- (positronium), e^-p (hydrogen), and μ^-p (muonic hydrogen) amplitudes. The one-photon exchange amplitude between the proton and the muon then leads to the Coulomb potential plus the fine and hyperfine structure (hfs), the Darwin term, and the retarded potentials [38,39]. The authors modified the standard Breit potential [9,43] for the μ^-p system with the inclusion of the electromagnetic form factors of the proton. The FSC to the Coulomb, Darwin, and fine and hyperfine energy levels for any n, l were provided, and an alternative expression for $\Delta E(= E^{f=1}_{2S_{1/2}} - E^{f=2}_{2P_{3/2}})$ was obtained by performing an expansion of the atomic wave functions. The main difference in their expression as compared to that of Ref. [7,8] arose due to the inclusion of the Darwin term with form factors. Since the use of a Dirac equation for energy levels would imply the inclusion of the Darwin term, the authors subtracted the point-like Darwin term from their calculations, leaving only the effect of this relativistic correction with form factors. They obtained

$$\Delta E(= E^{f=2}_{2P_{3/2}} - E^{f=1}_{2S_{1/2}}) = 209.16073 + 0.1174 r_p - 4.2585 r_p^2 + 0.0203 r_p^3 \text{ meV} \quad (12)$$

leading to a proton radius of r_p = 0.83594(46) fm, which was close to that obtained in Ref. [7,8] but hinted at an uncertainty introduced due to the use of a different FSC approach.

A brief discussion of the FSC in the hyperfine splitting is in order here. The FSC to the hyperfine splitting in Ref. [43] was evaluated using

$$\Delta E_{\text{hfs}} = \int |\Phi_C(\mathbf{r})|^2 \, \hat{V}_{\text{hfs}}(\mathbf{r}) d\mathbf{r} \quad (13)$$

where $\Phi_C(\boldsymbol{r})$ is the unperturbed hydrogen atom wave function. The spin operators are included in the definition of $\hat{V}_{\text{hfs}}(\boldsymbol{r})$ (see Ref. [27]). This correction seemed to be different from that used in Ref. [7,8], where it was calculated using the standard Zemach formula given by

$$\Delta E_{\text{hfs}} = -\frac{2}{3}\mu_1\mu_2 \langle \boldsymbol{\sigma}_1 \cdot \boldsymbol{\sigma}_2 \rangle \int |\Phi(\mathbf{r})|^2 \, f_{\text{m}}(\mathbf{r}) d\mathbf{r}, \quad (14)$$

where $f_m(\boldsymbol{r})$ is the Fourier transform of $G_M(\boldsymbol{q}^2)$. However, it was shown in Ref. [44] that Eqs. (13) and (14) would give the same result, provided we replace Φ_C by Φ in Eq. (13). Whereas $\Phi_C(\boldsymbol{r})$ in Eq. (13) is a solution of the point-like $1/r$ Coulomb potential, $\Phi(\boldsymbol{r})$ is the solution of the potential which includes the Coulomb potential with form factors and is given in Ref. [19] as $\Phi(\mathbf{r}) = \Phi_C(\mathbf{r}) + m_1 \alpha \Phi_C(0) \int f_{\text{e}}(\mathbf{u}) |\mathbf{u} - \mathbf{r}| d\mathbf{r}$. The difference therefore lies in the usage of the unperturbed wave function in the energy correction. In other words, in Refs. [43,44], the total Hamiltonian is taken as $H = H_0 + H^{FF}_C + H^{FF}_{\text{hfs}}$, with H_0 containing the $1/r$ Coulomb potential, H^{FF}_C, the FSC correction to the Coulomb potential, and H^{FF}_{hfs} the hyperfine interaction with form factors, leading to the energy correction in first-order perturbation theory given by $\Delta E_{\text{hfs}} = \langle \Phi_C | H^{FF}_C | \Phi_C \rangle + \langle \Phi_C | H^{FF}_{\text{hfs}} | \Phi_C \rangle$. In Ref. [19], one finds $H = \tilde{H}_0 + H^{FF}_{\text{hfs}}$, with $\tilde{H}_0$, which includes FSC to the Coulomb potential taken as the unperturbed Hamiltonian. We notice from the above discussion that the Breit equation and the Zemach method would lead to the same hyperfine correction if the time-independent perturbation theory were to be handled in the same way. In a calculation that involves FSC to the point-like Coulomb potential as well as hyperfine structure taken separately (as in Refs. [7,8,43]), it seems reasonable to use the prescription with $\Delta E_{\text{hfs}} = \langle \Phi_C | H^{FF}_C | \Phi_C \rangle + \langle \Phi_C | H^{FF}_{\text{hfs}} | \Phi_C \rangle$ in order to avoid double counting of the FSC to the Coulomb term. The r_p^2 and r_p^3 terms in Eqs. (9) and (12), for example, appear after the explicit inclusion of the FSC in the $(1/r)$ Coulomb potential.

The proton radius extracted from the muonic hydrogen Lamb shift is much more accurate than that determined from standard (electronic) hydrogen. The procedure of extracting the radius from electronic hydrogen is slightly different and involves a simultaneous determination of the Rydberg constant and the Lamb shift. Traditionally, the Lamb shift was actually a splitting (and not a shift) between the energy levels $E(2S_{1/2})$ and $E(2P_{1/2})$, which are degenerate according to the naive Dirac equation in the Coulomb field. The convention now, however, is to define the Lamb shift as any deviation from the prediction of the naive Dirac equation that arises from radiative, recoil, nuclear structure, relativistic, and binding effects (excluding hyperfine contributions) [45], so that $E_{njl} = E^{\text{Dirac}}_{nj} + L_{njl}$. The measurement of the Lamb shift can be disentangled from the Rydberg constant by using two different intervals of hydrogen structure. For example, we can use the accurate measurements of f_{1S-2S} = 2466061413187.34(84) kHz and $f_{2S1/2-8D5/2}$ =

770649561581.1(5.9) kHz, along with the energy expressions

$$E_{1S-2S}=\left[E^{\text{Dirac}}_{2S_{1/2}}-E^{\text{Dirac}}_{1S_{1/2}}\right]+L_{2S_{1/2}}-L_{1S_{1/2}}$$
$$E_{2S-8D}=\left[E^{\text{Dirac}}_{8D_{5/2}}-E^{\text{Dirac}}_{2S_{1/2}}\right]+L_{8D_{5/2}}-L_{2S_{1/2}} \quad (15)$$

to determine the radius. The first differences on the right-hand side are dependent on the Rydberg constant R_∞ (through $E^{\text{Dirac}}_{nj}=R_\infty E_{nj}$), which can be eliminated using the two equations. The left-hand side is replaced by accurate measurements, and the Lamb shift is determined independent of the Rydberg constant. Once the accurate value of the Lamb shift is known, this value can be inserted back into the above equations to determine the Rydberg constant accurately. The value of the Rydberg constant is thus obtained to be [5,6] R_∞=10973731.568539(55) m^{-1}. Knowing R_∞ accurately, one can now proceed to determine the radius as follows: Measured energy splitting = $R_\infty E_{nj}$+E(Lamb shift), where E(Lamb shift) includes all QED as well as proton structure corrections. With a good knowledge of all QED-related corrections (see for example Ref. [46,47]), the radius in the proton structure corrections appearing in E(Lamb shift) can be fitted to the measured energy splitting.

Reanalysis of scattering data

Apart from the various theoretical papers that attempted to explain the discrepancy between the proton radius from spectroscopy and scattering, there have also been some attempts at reanalyzing the *e-p* scattering data. We shall address some of the recent works and the related criticisms. In Ref. [48], the cross-sections at the lowest q^2 were fitted using two single-parameter models for form factors, with one being the standard dipole given by $G_E^{p2}(q^2)=(1+q^2/b_E)^{-4}$, $G_M^{p2}(q^2)/\mu_p^2=(1+q^2/b_M)^{-4}$ and the other involving a Taylor expansion given as $G_E^{p2}=1-c_E z$, $G_M^{p2}/\mu_p^2=1-c_E z$, where z is the conformal mapping variable as defined in Ref. [48]. Following the philosophy that the charge radius of the proton is a small-q^2 concept, the authors analyzed the low q^2 data using simple fits and reached the conclusion that the proton radius could vary between 0.84 and 0.89 fm, making the spectroscopy and scattering results consistent.

In a similar attempt, instead of focusing on a reanalysis of recent data, the authors decided to review the older Mainz and Saskatoon data [32]. They found that a dipole function with the muonic hydrogen radius of 0.84 fm (i.e., $G_E^p(q^2)=(1+q^2/0.66\ [\text{GeV}^2])^{-2}$) not only describes low q^2 $G_E^p(q^2)$ results but also reasonably describes $G_E^p(q^2)$ to the highest measured q^2. The authors in Refs. [49,50] performed a sharp truncation of the form factor expansion in momentum space, which was strongly criticized for not being in accord with the basic facts of form factors and the extraction of radii from them in Ref. [51].

A completely novel point of view was chosen in Ref. [13], where the authors noted that the proton radius may not be unique but may be a quantity that is randomly distributed over a certain range. The standard definition of a "radius" of the proton is obviously based on the notion of the proton being spherical. Arguing that the definition of the radius could become blurred for a deformed proton and providing other literature in support of the idea of a fluctuating size of the proton, the authors performed a fit for a form factor of the so-called "non-identical" protons. Taking the standard dipole form factor as the basis, the authors introduced the fluctuation of the proton size by performing an average with the following form:

$$\left\langle G_E^p(q^2,\Lambda_1)\right\rangle=\frac{1}{2\Delta\Lambda}\int_{\Lambda_1-\Delta\Lambda}^{\Lambda_1+\Delta\Lambda}G_E^p(q^2,\Lambda)\,d\Lambda \quad (16)$$

with the G_E in the integrand having the standard dipole form. The authors determined an average Λ_1 = 0.8203 GeV with a variation of 21.5% by using the latest Mainz data to perform the fits. They further studied the effects of such a radius variation in neutron star and symmetric nuclear matter. The electric form factor as defined in Eq. (16) can be evaluated analytically, and using Eq. (5) leads to a radius given by

$$r_p^2=\frac{12}{\Lambda_1^2-\Delta\Lambda^2}, \quad (17)$$

This, with the substitution of the values from [13], gives a proton radius r_p = 0.864 fm. Upon applying the relativistic correction (involving the Lorentz boost with λ_E = 1) in Ref. [14], the radius reduces to a value of 0.844 fm, which is quite close to that determined from muonic hydrogen spectroscopy [7,8]. In Fig. 1, we display the proton electric form factor at low momenta within the three different parametrizations discussed above. In Ref. [13], the authors investigated the density dependence of the proton radius in nuclear matter. The right panel in the Figure 1 shows the behavior of the proton radius using the parametrization in [13], with and without relativistic corrections (as found in Ref. [14]).

Brief overview of the planned experiments

The discussion of the proton radius puzzle has so far revolved around the extractions from *e-p* scattering measurements, standard hydrogen (electronic) spectroscopy, and muonic hydrogen spectroscopy. The missing component in these analyses is the data on muon-proton elastic

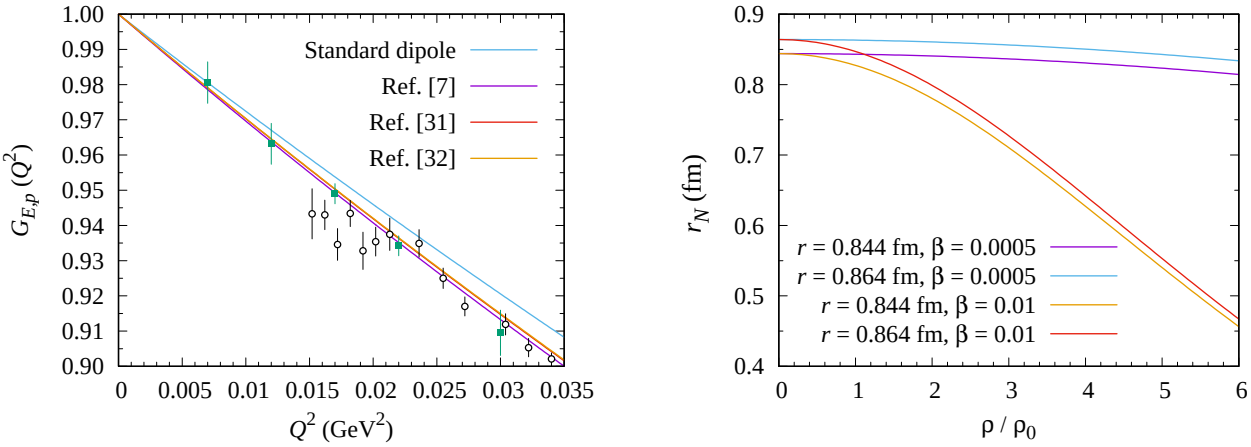

Figure 1. Comparison of the Parametrizations from Refs. [7, 31, 32] for Form Factors at Low $Q^2 = -q^2$ (Shown in the Left Panel). The Right Panel Displays the Density-dependent Proton Radius as Calculated in Ref. [7], with and without Relativistic Corrections Included

scattering. The MUon proton scattering experiment (MUSE) at the Paul Scherrer Institute is a simultaneous measurement of the μ^+p and e^+p elastic scattering. The experiment is expected to decide if the μp scattering and μ-p Lamb shift experiment lead to the same proton radius. Another scattering experiment is the PRad, which will measure the e-p scattering cross-sections with higher precision and at low q^2. In addition to these plans, the CREMA (Charge Radius Experiment with Muonic Atoms) collaboration has also been studying the spectroscopy of other exotic atoms, such as muonic deuterium and muonic helium. A detailed account of future experiments can be found in Refs. [17,18].

Conclusions

The finite size of the proton is characterized fully by all the moments of its charge distribution. The second moment is, however, generally used to define the "radius" of the proton. The radius thus defined can be extracted either from spectroscopic measurements or lepton proton scattering data using theoretical methods. Until some time ago, there seemed to be an agreement between the radii extracted from spectroscopy (with standard electronic hydrogen) and scattering. However, high-precision muonic hydrogen spectroscopy revealed a 4% deviation from the average value obtained from all previous experiments. Since the radius is an "extracted" and not directly "measured" quantity, a higher experimental precision should also be complemented by a higher confidence in the theoretical component. With this viewpoint, in this review we have examined the theoretical methods used for the extraction of the radius as well as the related literature that has offered possible solutions of the "proton radius puzzle." These included checks on the validity of the perturbative methods used and the approximations therein as well as the relevance of relativistic corrections. The latter is of particular importance due to the fact that the relation between the charge density and the electric form factor is necessarily of a non-relativistic nature. This fact also makes it important that the comparison of radii extracted from different experiments be done in the same frame of reference. While the resolution of the puzzle is being attempted by reanalyses of old data and planning of new experiments, it is equally necessary to pay attention to the theoretical inputs involved in the extraction of the radius.

Acknowledgements

T.M. was supported by the Research-Cluster-Grant-Program of the University of Indonesia, under Contract No. 1862/UN.R12/HKP.05.00/2015.

References

[1] Ernst, F.J., Sachs, R.G., Wali, K.C. 1960. Electromagnetic form factors of the nucleon. Phys. Rev. 119: 1105-1114, doi: 10.1103/PhysRev.119.1105.

[2] Bosted, P.E., Andivahis, L., Lung, A., Stuart, L.M., Alster, J., Arnold, R.G., Chang, C.C., Dietrich, F.S., Dodge, W., Gearhart, R., Gomez, J., Griffioen, K.A., Hicks, R.S., Hyde-Wright, C.E., Keppel, C., Kuhn, S.E., Lichtenstadt, J., Miskimen, R.A., Peterson, G.A., Petratos, G.G., Rock, S.E., Rokni, S., Sakumoto, W.K., Spengos, M., Swartz, K., Szalata, S., Tao, L.H. 1992. Measurements of the electric and magnetic form factors of the proton from Q^2 = 1.75 to 8.83 (GeV/c)^2. Phys. Rev. Lett. 68: 3841-3844, doi: 10.1103/PhysRevLett.68.3841.

[3] Friedrich, J., Walcher, Th. 2003. A coherent interpretation of the form-factors of the nucleon in

terms of a pion cloud and constituent quarks. Eur. Phys. J. A17: 607-623, doi: 10.1140/epja/i2003-10025-3

[4] Perdrisat, C.F., Punjabi, V., Vanderhaeghen, M. 2007. Nucleon electromagnetic form factors. Prog. Part. Nucl. Phys. 59: 694-764, doi: 10.1016/j.ppnp. 2007.05.001.

[5] Mohr, P.J., Taylor, B.N., Newell, D.B. 2003. CODATA recommended values of the fundamental physical constants: 2006. Rev. Mod. Phys. 80: 633-730, doi: 10.1103/RevModPhys.80.633.

[6] Mohr, P.J., Taylor, B.N., Newell, D.B. 2012. CODATA recommended values of the fundamental physical constants: 2010. Rev. Mod. Phys. 84: 1527-1605, doi: 10.1103/RevModPhys.84.1527.

[7] Antognini, A., Nez, F., Schuhmann, K., Amaro, F.D., Biraben, F., Cardoso, J.M.R., Covita, D.S. 2013. Proton structure from the measurement of 2S−2P transition frequencies of muonic hydrogen. Science 339(6118): 417-420, doi: 10.1126/science. 1230016.

[8] Pohl, R., Antognini, A., Nez, F., Amaro, F.D., Biraben, F., Cardoso, J.M.R., Covita, D.S., Dax, A., Dhawan, S., Fernandes, L.M.P., Giesen, A., Graf, T., Hansch, T.W., Indelicato, P., Julien, L., Kao, C.Y., Knowles, P., Le Bigot, E.O., Liu, Y.W., Lopes, J.A.M., Ludhova, L., Monteiro, C.M.B., Mulhauser, F., Nebel, T., Rabinowitz, P., Santos, J.M.F., Schaller, L.A., Schuhmann, K., Schwob, C., Taqqu, D., Veloso, J.F.C.A., Kottmann, F. 2010. The size of the proton. Nature. 466: 213-216, doi: 10.1038/nature09250.

[9] Kelkar, N.G., Daza, F.G., Nowakowski, M. 2012. Determining the size of the proton. Nucl. Phys. B864: 382-398, doi: 10.1016/j.nuclphysb.2012.06.015.

[10] Miller, G.A., Thomas, A.W., Carroll, J.D., Rafelski, J. 2011. Natural resolution of the proton size puzzle. Phys. Rev. A 84: 020101(R), doi: 10.1103/PhysRevA.84.020101.

[11] Miller, G.A. 2013. Proton polarizability contribution: muonic hydrogen Lamb shift and elastic scattering. Phys. Lett. B718: 1078-1082, doi: 10.1016/j.physletb. 2012.11.016.

[12] Sick, I. 2012. Problems with proton radii. Prog. Part. Nucl. Phys. 67: 473-478, doi: 10.1016/j.ppnp. 2012.01.013.

[13] a. Mart, T., Sulaksono, A. 2013. Nonidentical protons. Phys. Rev. C87: 025807, doi:10.1103/ PhysRevC.87.025807. b. Mart, T., Sulaksono, A. 2013. Reply to "Comment on 'Nonidentical protons' ". Phys. Rev. C88: 059802, doi:10.1103/ PhysRevC.88.059802. c. Mart, T., Sulaksono, A. 2016. Reply to "Comment on 'Nonidentical protons' ". Phys. Rev. C93: 039802, doi:10.1103/ PhysRevC.93.039802.

[14] Fierro, D.B., Kelkar, N.G., Nowakowski, M. 2015. Lorentz contracted proton. J. High Energy Phys. 2015(9):1-15, doi: 10.1007/JHEP09(2015)215.

[15] Robson, D. 2014. Solution to the proton radius puzzle. Int. J. Mod. Phys. E 23: 1450090, doi: 10.1142/S0218301314500906

[16] Giannini, M.M., Santopinto, E. 2013. On the proton radius problem. Preprint arXiv: 1311.0319.

[17] Carlson, C.E. 2015. The proton radius puzzle. Prog. Part. Nucl. Phys. 82: 59-77, doi: 10.1016/ j.ppnp.2015.01.002.

[18] Antognini, A., Schuhmann, K., Amaro, F.D., Amaro, P., Abdou-Ahmed, M., Biraben, F., Chen, T.-L., Covita, D.S., Dax, A.J., Diepold, M., Fernandes, L.M.P., Franker, B., Galtier, S., Gouvea, A.L., Gotzfried, J., Graf, T., Hansch, T.W., Hildebrandt, M., Indelicato, P., Julien, L., Kirch, K., Knecht, A., Kottmann, F., Krauth, J.J., Liu, Y.-W., Machado, J., Monteiro, C.M.B., Mulhauser, F., Nez, F., Santos, J.P., dos Santos, J.M.F., Szabo, C.I., Taqqu, D., Veloso, J.F.C.A., Voss, A., Weichelt, B., Pohl, R. 2016. Experiments towards resolving the proton charge radius puzzle. EPJ Web Conf. 113: 01006, doi: 10.1051/epjconf/ 201611301006.

[19] Zemach, A.C. 1956. Proton structure and the hyperfine shift in hydrogen. Phys. Rev. 104: 1771-1781, doi: 10.1103/PhysRev.104.1771.

[20] De Rújula, A. 2011. QED confronts the radius of the proton. Phys. Lett. B697: 26-31, doi: 10.1016/ j.physletb.2011.01.025

[21] De Rujula, A. 2010. QED is not endangered by the proton's size. Phys. Lett. B693(5): 555-558, doi: 10.1016/j.physletb.2010.08.074.

[22] Cloët, I.C., Miller, G.A. 2011. Third Zemach moment of the proton. Phys. Rev. C83: 012201(R), doi: 10.1103/PhysRevC.83.012201.

[23] Friar, J.L., Sick, I. 2005. Muonic hydrogen and the third Zemach moment. Phys. Rev. A72: 040502(R), doi: 10.1103/PhysRevA.72.040502.

[24] Vanderhaeghen, M., Walcher, T. 2011. Long range structure of the nucleon. Nucl. Phys. News. 21: 14-22, doi: 10.1080/10619127.2011.554757.

[25] Bernauer, J.C., Distler, M.O., Friedrich, J. Walcher, Th., Achenbach, P., Gayoso, A., Böhm, R., Bosnar, D., Debenjak, L., Doria, L., Esser, A., Fonvieille, H., Gómez Rodríguez de la Paz, M., Friedrich, J.M. Makek, M., Merkel, H., Middleton, D.G., Müller, U., Nungesser, L., Pochodzalla J., Potokar, M., Sánchez Majos, S., Schlimme, B.S., Širca, S., Weinriefer, M. 2014. Electric and magnetic form factors of the proton. Phys. Rev. C90: 015206, doi: 10.1103/PhysRevC. 90.015206.

[26] Eides, M.I. 2014. Recent ideas on the calculation of lepton anomalous magnetic moments. Phys. Rev. D90: 057301, doi: 10.1103/PhysRevD.90. 057301.

[27] Kelly, J.J. 2002. Nucleon charge and magnetization densities from Sachs form-factors. Phys. Rev. C66: 065203, doi: 10.1103/PhysRevC.66.065203.

[28] Licht, A.L., Pagnamenta, A. 1970. Wave functions and form-factors for relativistic composite particles.

II. Phys. Rev. D2: 1156-1160, doi: 10.1103/PhysRevD.2.1156.
[29] Holzwarth, G. 1996. Electromagnetic nucleon form-factors and their spectral functions in soliton models. Z. Phys. A356: 339-350, doi: 10.1007/s002180050187.
[30] Holzwarth, G. 2005. Electromagnetic form-factors of the nucleon in chiral soliton models. hep-ph/0511194.
[31] Mitra, A.N., Kumari, I. 1977. Relativistic form-factors for clusters with nonrelativistic wave functions. Phys. Rev. D15: 261-266, doi: 10.1103/PhysRevD.15.261.
[32] Beachey, D.J., Nogami, Y., Toyama, F.M., van Dijk, W. 1994. The relation between the form factor and the radius of the deuteron: relativistic effects. J. Phys. G 20: L143-L147, doi: 10.1088/0954-3899/20/12/002.
[33] Friar, J.L. 1979. Nuclear finite-size effects in light muonic atoms. Ann. Phys. 122: 151-196, doi: 10.1016/0003-4916(79)90300-2.
[34] Antognini, A., Kottmann, F., Biraben, F., Indelicato, P., Nez, F., Pohl, R. 2013. Theory of the 2S–2P Lamb shift and 2S hyperfine splitting in muonic hydrogen. Ann. Phys. 331: 127-145, doi: 10.1016/j.aop.2012.12.003.
[35] Carlson, C.E., Vanderhaeghen, M. 2011. Higher order proton structure corrections to the Lamb shift in muonic hydrogen. Phys. Rev. A84: 020102, doi: 10.1103/PhysRevA.84.020102.
[36] Carroll, J.D., Thomas, A.W., Rafelski, J., Miller, G.A. 2011. Nonperturbative relativistic calculation of the muonic hydrogen spectrum. Phys. Rev. A84(1): 1-11, doi: 10.1103/PhysRevA.84.012506.
[37] Pang, H.R., Zhou, H.Q. 2015. Nonperturbative numerical calculation of the fine and hyperfine structure of muonic hydrogen by Breit potential including the effects from the proton size. Cornell University Library. Preprint arXiv: 1504.06940.
[38] Bethe, H.A., Salpeter, E.E. 2008. Quantum mechanics of one- and two-electron atoms. Dover. New York. pp. 4-118.
[39] Berestetskii, V.B., Lifshitz, E.M., Pitaevskii, L.P. 2007. Quantum electrodynamics, Landau-Lifshitz course on theoretical physics Vol.4, 2nd ed. Oxford. Butterworth-Heinemann. p. 652.
[40] De Sanctis, M., Quintero, P. 2010. Charmonium spectrum with a generalized Fermi-Breit equation. Eur. Phys. J. A 46: 213-221, doi: 10.1140/epja/i2010-11032-y.
[41] De Sanctis, M. 2009. A generalization of the Fermi-Breit equation to non-Coulombic spatial interactions. Eur. Phys. J. A41: 169-178, doi: 10.1140/epja/i2009-10823-5.
[42] De Sanctis, M. 2014. A relativistic wave equation with a local kinetic operator and an energy-dependent effective interaction for the study of hadronic systems. Central Eur. J. Phys. 12: 221-232, doi: 10.2478/s11534-014-0444-0.
[43] Daza, F.G., Kelkar, N.G., Nowakowski, M. 2012. Breit Equation with form factors in the hydrogen atom. J. Phys. G 39: 035103, doi: 10.1088/0954-3899/39/3/035103.
[44] Kelkar, N.G., Nowakowski, M., Bedoyo Fierro, D. 2014. Opportunities and problems in determining proton and light nuclear radii. Pramana 83: 761-771, doi: 10.1007/s12043-014-0875-6.
[45] Eides, M.I., Grotch, H., Shelyuto, V.A. 2001. Theory of light hydrogen-like atoms. Phys. Rep. 342: 63-261, doi: 10.1016/S0370-1573(00)00077-6.
[46] Martynenko, A.P. 2005. 2S hyperfine splitting of muonic hydrogen. Phys. Rev. A71: 022506, doi: 10.1103/PhysRevA.71.022506.
[47] Martynenko, A.P. 2008. Fine and hyperfine structure of P-levels in muonic hydrogen. Phys. Atom. Nucl. 71: 125-135, doi: 10.1134/S1063778808010146.
[48] Horbatsch, M., Hessels, E.A. 2016. Evaluation of the strength of electron-proton scattering data for determining the proton charge radius. Phys. Rev. C 93: 015204, doi: 10.1103/PhysRevC.93.015204.
[49] Higinbotham, D.W., Kabir, A.A., Lin, V., Meekins, D., Norum, B., Sawatzky, B. 2016. Proton radius from electron scattering data. Phys. Rev. C93: 055207, doi: 10.1103/PhysRevC.93. 055207.
[50] Griffioen, K., Carlson, C., Maddox, C. 2015. Are electron scattering data consistent with a small proton radius? Preprint arXiv:1509.06676.
[51] Distler, M.O., Walcher, T., Bernauer, J.C. 2015. Solution of the proton radius puzzle? Low momentum transfer electron scattering data are not enough. Preprint arXiv:1511.00479.